Solar-driven electrochemical nitrate reduction to ammonia catalyzed by nickel cobalt oxide-palladium heterojunction

Fenglin Zhao[a], Jingru Zhou[a], Zhengqin Sun[a], Yitong Li[a], Yingge Zhang[a], Qin Hu[a], Chunlin Liu[a, *], Haifeng Jiang[b, *], Xiaodong Zhu[a, *]

[a] School of Mechanical Engineering, Chengdu University, Chengdu 610106, China

[b] College of Chemistry, Beijing University of Chemical Technology, Beijing 100029, China

*Corresponding Authors.

E-mail: liuchunlin@cdu.edu.cn (C. Liu), 2025500093@buct.edu.cn (H. Jiang), xiaodangjia21@126.com (X. Zhu)

Membrane electrode assembly electrolyzer measurements

The flow electrolyzer was assembled with two stainless-steel cover plates. 1 M KOH + 0.1 M KNO_3 and 1 M KOH were supplied as cathodic and anodic electrolytes, respectively. And the electrolyte was conveyed by peristaltic pumps with a flow rate of 25.7 mL h^{-1}. $NiFeO_x$ is purchased from SINERO (1 mg cm^{-2}). The solar power generation panel is purchased from Xiangri Crop. (SUNNY, SYSP), and is matched with an adjustable step-down power supply module to ultimately achieve various constant voltage outputs. Other parameters of solar-driven are the same as those of the aforementioned flow electrolyzer.

Quantification of anion concentration

The concentration of ammonia, nitrite, and nitrate was measured via colorimetry by ultraviolet-visible spectroscopy. The anion concentration of these pre-test or post-test electrolytes is analyzed after diluting to a specific concentration, which falls within the range of calibration curves.

Determination of NH_3. The concentration of NH_3 in aqueous electrolyte was obtained by the indophenol blue method as follows. Solution α: 40 mL H_2O, 1.6 g NaOH, 2 g sodium citrate, and 2 g salicylic acid. Solution β: 10 mL H_2O and 0.506 mL $NaClO_4$. Solution γ: 10 mL H_2O and 0.1 g nitroferricyanide solution. Typically, 2 mL diluted post-test electrolyte, 2 mL solution α, 1 mL solution β, and 200 μL solution γ were thoroughly mixed and let sit for another hour. Then, the solution absorbance was detected at 658 nm using a UV-vis spectrophotometer.

Determination of nitrate. Firstly, 0.1 M HCl and 0.8 wt.% sulfamic acid aqueous solution were prepared. Then, 2 mL H_2O, 2 mL diluted electrolyte, 100 μL HCl, and 10 μL sulfamic acid were fully mixed. Let it sit for twenty minutes. Then it was detected by a UV-vis spectrophotometer in the range of 200 ~ 300 nm.

Determination of nitrite. Firstly, 2.0 g of sulfonamide, 0.2 g of N-(1-naphthyl)ethyldiamine dihydrochloride, and 5.88 mL of phosphoric acid were mixed in 100 mL of H_2O and finally named as Griess reagent. Then, 2 mL H_2O, 1 mL diluted

electrolyte, and 1 mL Griess reagent were wholly mixed. Let it sit for fifty minutes. Then it was detected by a UV-vis spectrophotometer in the range of 500 ~ 600 nm.

Operando reflection Fourier transform infrared (FTIR) measurements

Operando FTIR was conducted on the Bruker INVENIO-S of attenuated total reflectometry equipped with the MCT-A detector system, which was applied in combination with an electrochemical workstation (Chenhua 760E). The catalytic material was deposited on a silicon crystal for testing. The electrochemical testing procedure remained largely consistent with the conventional protocol except for the electrolyte. To enhance the intensity of FTIR absorbance, the cathodic electrolyte was chosen as 0.1 M Na_2SO_4 and 0.5 M KNO_3. Prior to each infrared measurement, a chronoamperometry test was applied for 5 minutes (−0.1 ~ −0.9 V vs. RHE).

^{15}N Isotope Labeling Experiments

To uncover the source of ammonia, 99% $K^{15}NO_3$ was utilized as the feeding N-reactant. Except for ^{14}N being replaced by ^{15}N, the other reaction conditions of NO_3RR remain unchanged (the reaction potential is −0.8V vs. RHE). Take 500 μL of the post-reaction electrolyte, adjust its pH to 2 with 1 M HCl, and add 100 μL of dimethyl sulfoxide-d_6 solution. After thorough mixing, the sample solution is obtained. Finally, the nuclear magnetic resonance (NMR) spectrum was acquired using the PRESAT mode for water-suppressed ^{1}H NMR.

Computational Details

All these calculations were carried out using Vienna Ab initio Simulation Package with the projector augmented wave process, where the exchange-functional was described within the generalized gradient approximation through Perdew-Burke-Emzerhof formulation [1-3]. A plane-wave basis energy cutoff of 450 eV was adopted, and geometry optimization was considered converged as the force on the atom was below 0.05 eV/Å. The technique of Grimme's DFT-D3 was utilized to account for dispersion interactions [4]. The Kohn-Sham orbital partial occupancy was permitted through a Gaussian smearing process within a width of 0.05 eV. The Brillouin zone

was partitioned with Monkhorst mesh 2× 2 × 1 throughout all calculations. The self-consistent field convergence basis was set to 10^{-5} eV. $NiCo_2O_4$ exhibits the (110) crystal plane, whereas Pd presents the (111) plane, as determined by our calculations. The NO_3RR free energy is calculated by the equation: $\Delta G = \Delta E_{DFT} + \Delta E_{ZPE} - T\Delta S$. Where ΔE_{DFT} represents DFT electronic energy variance of each step, ΔE_{ZPE} represents the correction of zero-point energy, ΔS represents he variation of entropy, and T is the temperature (300 K).

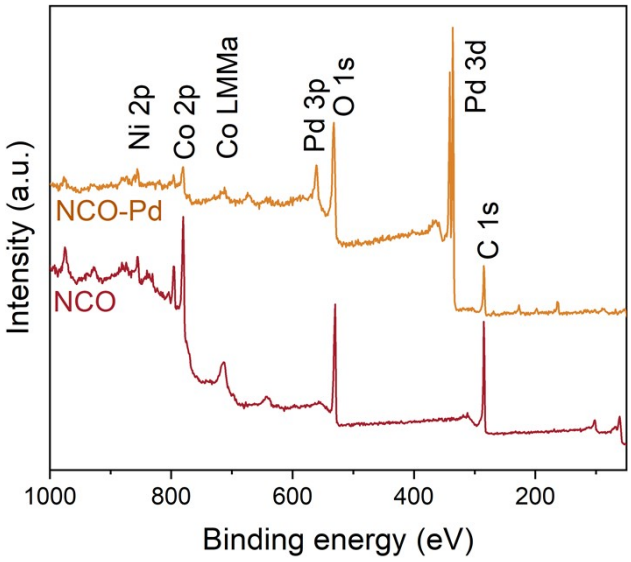

Fig. S1. XPS survey spectra of NCO and NCO-Pd.

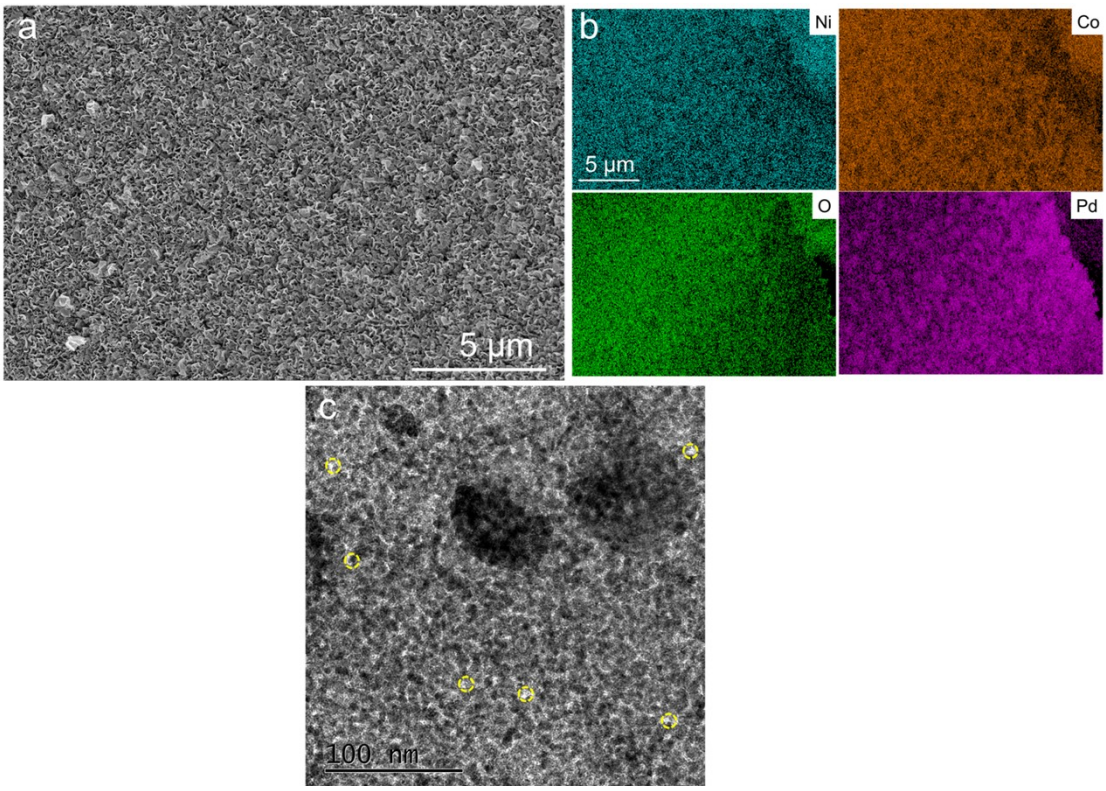

Fig. S2. (a) SEM image of NCO, (b) elemental distribution of NCO-Pd. (c) TEM image of NCO-Pd, where only a few representative holes are depicted in the figure.

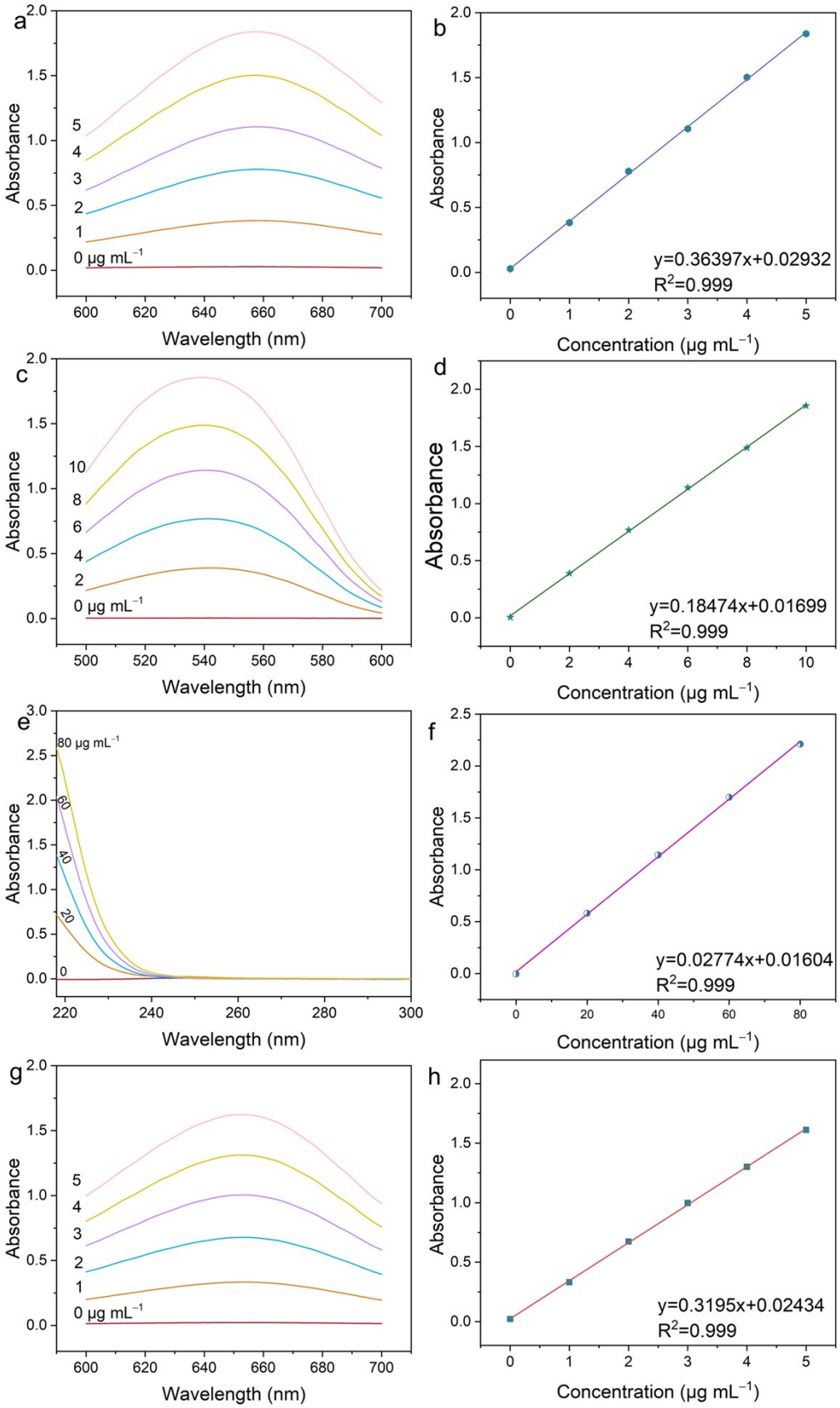

Fig. S3. UV-Vis absorbance spectra and the corresponding calibration plots for calculating the ammonia (a, b), nitrite (c, d), and nitrate (e, f) of various concentrations, and the ammonia (g, h) in 1M KOH solution.

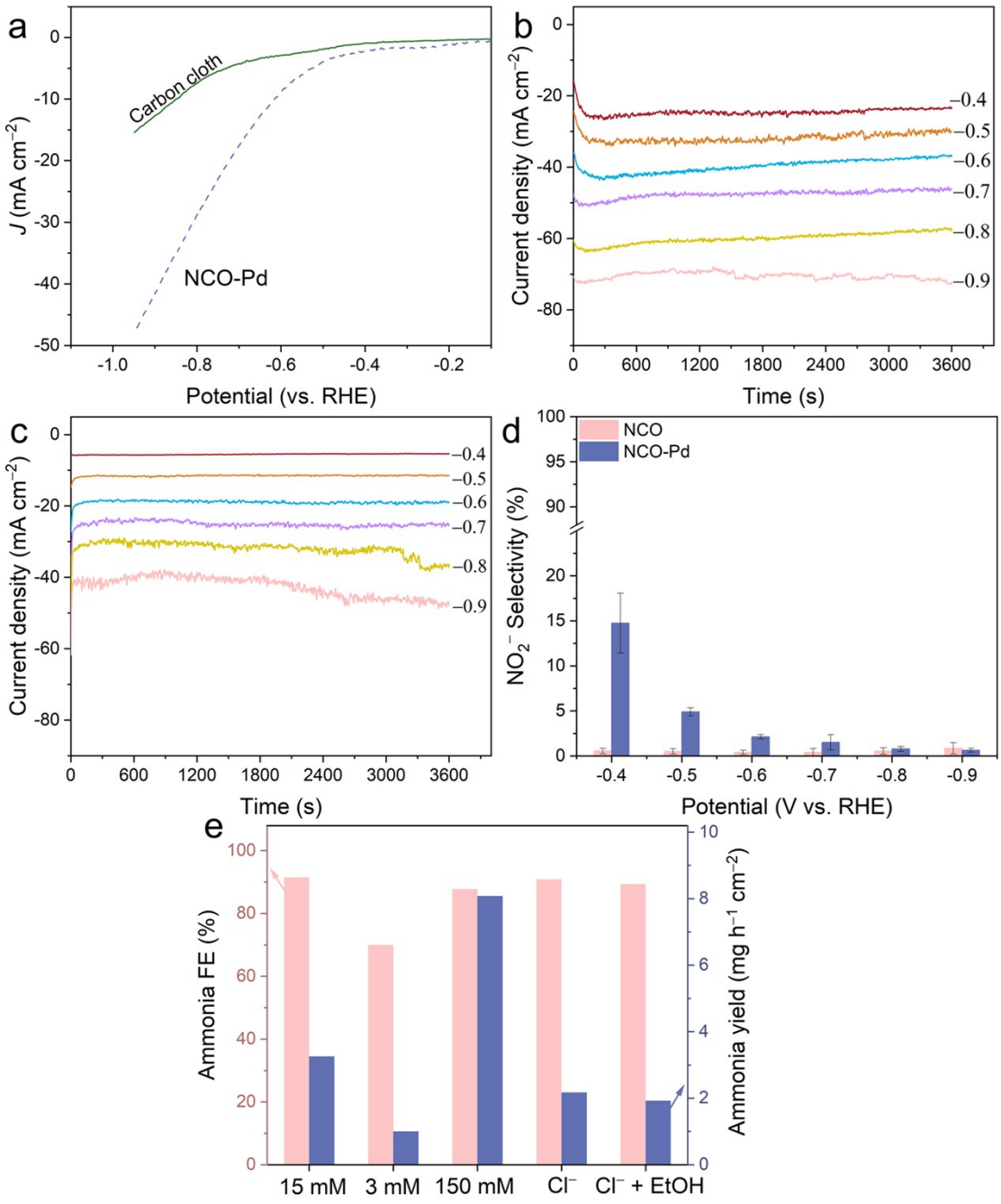

Fig. S4. (a) LSV curve of the catalyst based on carbon cloth, and the dashed line indicates the electrocatalysis of NCO-Pd catalyzed in Na_2SO_4 electrolyte. Chronoamperometry test curves at various potentials for NO_3RR of (b) NCO-Pd and (c) NCO. (d) Nitrite selectivity of NCO and NCO-Pd. (e) The ammonia yield and FE of NCO-Pd under various electrolyte scenarios in 0.1 M Na_2SO_4, where 15 mM represents 15 mM KNO_3, 3 mM represents 3 mM KNO_3, 150 mM represents 150 mM KNO_3, Cl^- represents 5 mM KCl, and Cl^- + EtOH represents 5 mM KCl + 34 mM EtOH.

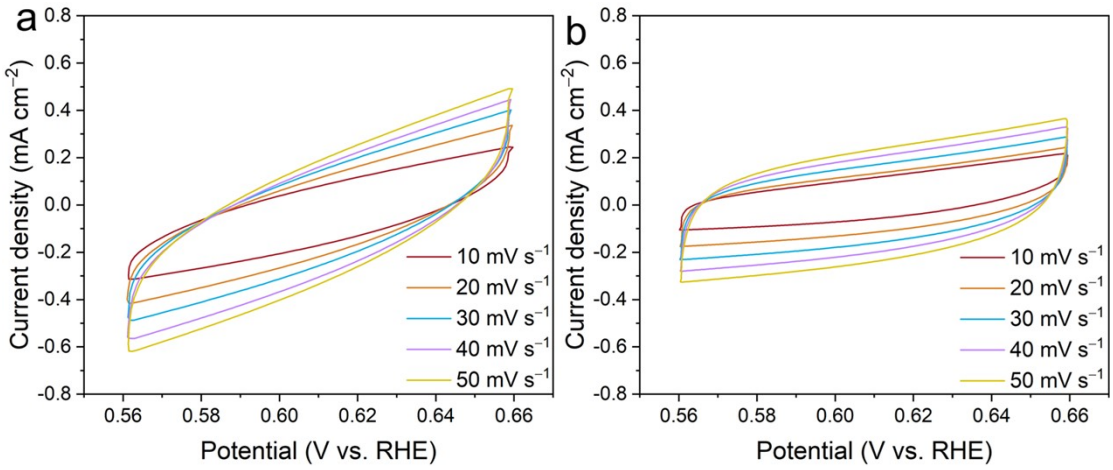

Fig. S5. CV curves of (a) NCO and (b) NCO-Pd over NO3RR at the scan rate of from 10 to 50 mV s^{-1}.

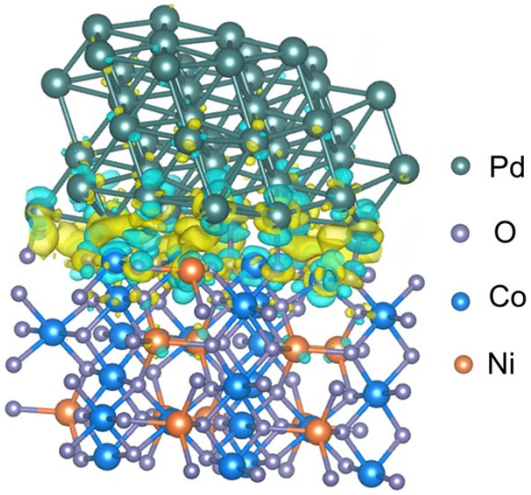

Fig. S6. Charge density difference of the NCO-Pd heterostructure interface (yellow color stands for charge accumulation and blue color represents depletion).

Table S1. The electrocatalytic NO_3RR properties have been compared with those of several similar catalysts in neutral electrolytes over the past two years.

Catalysts	Yield rate (mmol $h^{-1}cm^{-2}$)	FE	Electrolyte	Reference
$CoMn_2O_4$/NC	0.06	92.4%	0.1 M Na_2SO_4 +0.1 M KNO_3	*Appl. Catal. B Environ., 322 (2023) 122090*
δ-FeOOH	0.34	90.2%	0.25 M PBS + 500 ppm NO_3^-	*Small 2024, 20, 2401327*
Co_3O_4-Ov	0.26	88.1%	0.1 M Na_2SO_4 + 0.016 M KNO_3	Chem. Eng. J. 461 (2023) 141960
Cu1Co1–BCN	0.377	92.4%	0.1 M PBS + 0.1 M KNO_3	*J. Mater. Chem. A 2023, 11, 20234*
Co@Cu NW	0.30	88.6%	0.5 M Na_2SO_4 + 0.1 M NO_3^-	*ACS Catal. 2024, 14, 22, 17046–17054*
VO_{2-x}/CuF	1.833	77.9%	0.1 M K_2SO_4 + 0.1 M KNO_3	J. Power Sources 608 (2024) 234644
FeSA/Mxene	0.58	82.9%	0.1 M Na_2SO_4 + 0.5 M $NaNO_3$	*Environ. Sci. Technol. 2023, 57, 10458*
NiFe−LDH	0.21	90.1%	0.05 M Na_2SO_4 + 0.05 M $NaNO_3$	*ACS Catal. 2025, 15, 6918−6928*
RuP_2-MnP	1.67	89.6%	0.1 M K_2SO_4 + 0.1 M KNO_3	*Electrochimica. Acta 536 (2025) 146747*
COF-366-Fe	1.884	85.4%	0.5 M Na_2SO_4 + 0.1 M KNO_3	*Adv. Energy Mater. 2024, 14, 2302608*
NiFe−LDH	0.21	90.1%	0.05 M Na_2SO_4 + 50 mM $NaNO_3$	*ACS Catal. 2025, 15, 6918−6928*
NCO-Pd	0.194	91.2%	0.1 M Na_2SO_4 + 15 mM KNO_3	Our work

References

1. G. Kresse, J. Furthmüller, Comput. Mater. Sci. 1996, **6**, 15-50.
2. P.E. Blöchl, Phy. Rev. B, 1994, **50**, 17953-17979.
3. J.P. Perdew, J.A. Chevary, S.H. Vosko, K.A. Jackson, M.R. Pederson, D.J. Singh, C. Fiolhais, Phy. Rev. B, 1992, **46**, 6671-6687.
4. S. Grimme, J. Antony, S. Ehrlich, H. Krieg, J. Chem. Phys.2010, **132**, 154104.